Proceedings of the 16th Czech and Slovak Conference on Magnetism, Košice, Slovakia, June 13–17, 2016

The Influence of Preparation Methods on Magnetic Properties of Fe/SiO_2 Soft Magnetic Composites

J. Füzerová[a,*], J. Füzer[b], P. Kollár[b], M. Kabátová[c] and E. Dudrová[c]

[a]Department of Applied Mathematics and Informatics, Faculty of Mechanical Engineering, Technical University Košice, Letná 1, 042 00 Košice, Slovakia

[b]Institute of Physics, Faculty of Sciences, P.J. Šafárik University, Park Angelinum 9, 041 54 Košice, Slovakia

[c]Institute of Materials Research, Slovak Academy of Sciences, Watsonova 47, 040 01 Košice, Slovak Republic

An analysis of several variants of the Fe/polymer/SiO_2 composites in terms of the impact of iron powder particle shape (irregular, spherical), of the content (0.4–2.0 wt%), of the polymer type (shellac, thermoset SL450) and the method of its application as well as the effect of the preparation procedure of the composites (mixing and/or vacuum-pressure impregnation) on properties of electrical insulating layer (thickness and coherence), electrical resistivity and magnetic properties was carried out. It was found that the main governing factor of the microstructure formation is the shape, surface microgeometry of the iron particles and the insulator layer. These determine not only the uniformity of thickness and cohesion of the insulating layer of the applied polymer or its hybrid modification (polymer+SiO_2 nanoparticles), but also the most suitable method of preparation in terms of the achieved values of electrical and magnetic properties of the composites.

DOI: 10.12693/APhysPolA.131.816

PACS/topics: 75.50.Bb, 85.70.–w, 81.05.Ni

1. Introduction

Soft magnetic composites (SMCs) offer an interesting alternative to the traditional laminated silicon iron sheets as core material in electrical machines. SMCs are mostly composed of pure iron powder particles insulated from each other by organic or inorganic material, which insulates and binds ferromagnetic particles and produces a high electrical resistivity [1]. Extremely important is the insulating phase which determines the density, mechanical properties, electrical resistivity and essentially all magnetic properties of SMCs [2, 3]. Different thermosets are mostly applied as organic insulation [1, 4] and as inorganic insulation phase, the $FePO_4$, MgO and SiO_2 compounds are most commonly used [5–7]. In the present study, the effect of the iron particle shape, way of adding SiO_2 and the effect of polymer type used to the nature of the insulating layer was investigated focusing on the complex permeability spectra, the DC and AC total magnetic losses. The aim of this work was to choose the best samples from 24 variants of the Fe/polymer/SiO_2 composites in our previous work [8] for magnetic characterization from the comprehensive analysis

2. Experimental

Fe/(0.4–2 wt%)SiO_2/polymer composite materials are based on iron powder particles irregularly and/or spherically shaped, the SiO_2 component was added as a nanopowder. Ring and cylindrical composite samples were prepared by powder metallurgy, conventional mixing the Fe/SiO_2 powder with shellac dissolved in ethanol and by an unconventional vacuum/pressure impregnation procedure (VPI) of low-temperature sintered Fe/SiO_2 compacts with shellac dissolved in ethanol. Powder mixtures were dried at room temperature for 60 min in air and subsequently cold compacted at pressure of 800 MPa into cylindrical and rings compacts, respectively. More details concerning experimental procedure were published in our previous works [8, 9]. Microscopic observation was performed using light and scanning electron microscopy (Olympus GX71, Jeol-JSM-7000F coupled with EDX INCA analyser). The cylinder samples were used for measurement of coercivity by Foerster Koerzimat 1.097 HCJ and for measurement of specific electrical resistivity by the Van der Pauw method. The densities were evaluated by dimensions measurements and mass of the sintered bodies. The impedance bridge (HP4194A) was used for complex permeability measurement in the frequency range from 800 Hz to 40 MHz. The AC hysteresis loops were measured in the frequency range 2–22 kHz by MATS-2010SA hysteresis graph at the maximum flux density of 0.1 T.

3. Results and discussion

The formulation of the prepared composites and processing conditions used, are as follows: Mix A and Mix B have irregular 30−160 μm iron particles, without (A) or with 2 wt% (B) of SiO_2 nano-powder, are mixed with 1 (A) or 2% (B) of shellac, compacted, and cured at 100 °C/20min/air; VPI A, VPI B, VPI C, and VPI D have irregular 30−160 μm (A and D) or spherical 100−160 μm (B and C) iron particles, are mixed with 0.4 wt% (A and B) or 2 wt% (C and D) of SiO_2

*corresponding author; e-mail: jana.fuzerova@gmail.com

nano-powder, compacted, sintered at 850 °C, and vacuum/pressure impregnated (VPI) with 1% shellac. It is known that the first stage of the compacting of powder is associated with the redistribution of powder particles by shifting and rotation with subsequent development of plastic deformation in the areas of particle contacts. In the case of irregularly shaped iron particles with numerous protrusions at the surface, creation of Fe/Fe contacts may occur due to the breach of the electrical insulating layer. The micrographs of Mix A sample show a good adhesion of shellac to iron particle surfaces but the thickness of the insulating layer is uneven, Fig. 1. The micrographs of Mix B sample show that the thickness of insulating layer consisting of SiO_2 coating and shellac is uneven and relatively thick, Fig. 2.

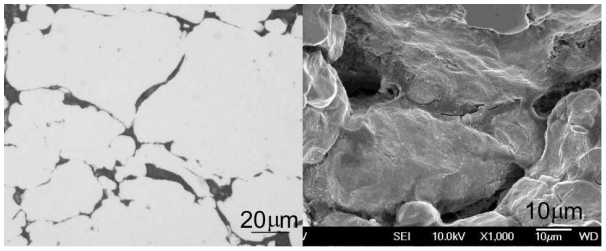

Fig. 1. Microstructure and fracture surface of the Mix A sample.

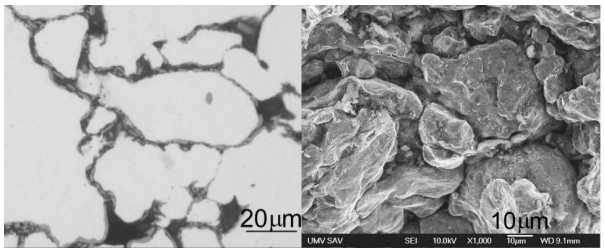

Fig. 2. Microstructure and fracture surface of the Mix B sample.

The insulating layer of the VPI A sample seems to be continuous, but with an uneven thickness. Some small metallic connections were formed in the "protrusions" on iron particle surface during pre-sintering, Fig. 3. The micrographs of VPI B sample show the formation of thin and continuous electrical insulating layer (shellac+SiO_2 nanopowder) with uniformly distributed SiO_2 nanoparticles, Fig. 4. More details concerning the fracture surfaces were published in works [8–10].

Table I shows a comparison of specific electrical resistivity and coercivity of the prepared samples. A wide range of values achieved for the electrical resistivity is a result of the common effect of a number of factors related to iron powder properties as well as to those acting during the preparation of the composite. The results showed that composites with a low electrical resistance exhibit also low coercivity.

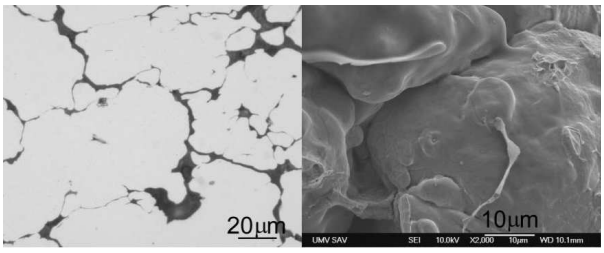

Fig. 3. Microstructure and fracture surface of the VPI A sample.

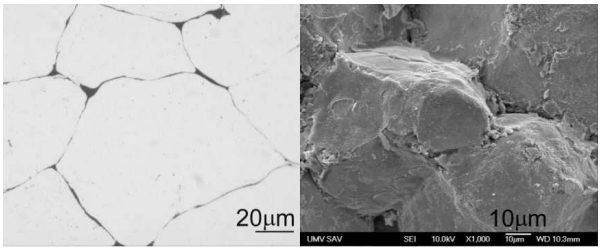

Fig. 4. Microstructure and fracture surface of the VPI B sample.

The frequency dependences of the real and the imaginary part of complex permeability are shown in Fig. 5 and Fig. 6. The lower (0.4 wt%) content of SiO_2 as electrically insulating layer between particles of composite is leading to steep decrease of the real part of complex permeability beyond 1500 Hz. However these samples (VPI A and VPI B) have the highest value of the real part of complex permeability (68 and 75, respectively at 1 kHz).

For all other samples the real part of complex permeability exhibits stable behaviour up to higher frequencies. Near-to-constant at least up to 200 kHz is real permeability for samples Mix A and Mix B. The imaginary part of complex permeability is illustrated in Fig. 6. The relaxation frequency is attributed to the peak of the imaginary part. For VPI A and VPI B samples it is located at low frequency (4 kHz). In case of Mix A and Mix B samples the peaks can be seen at around 2 MHz. With the increasing electrical resistivity the peak is shifting to higher frequencies.

TABLE I

The values of specific electrical resistivity and coercivity of prepared samples.

Sample	Resistivity [$\mu\Omega$m]	Coercivity [A/m]
Mix A	1760	405
Mix B	4100	425
VPI A	0.365	175
VPI B	0.119	180
VPI C	216	300
VPI D	95	295

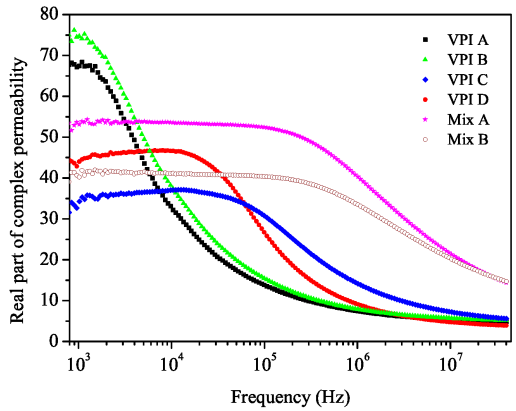

Fig. 5. The dependence of real part of complex permeability on frequency.

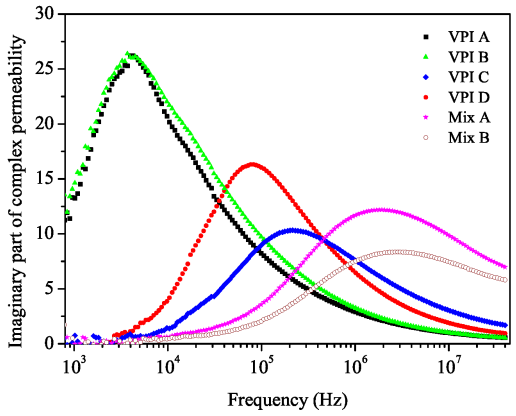

Fig. 6. The dependence of imaginary part of complex permeability on frequency.

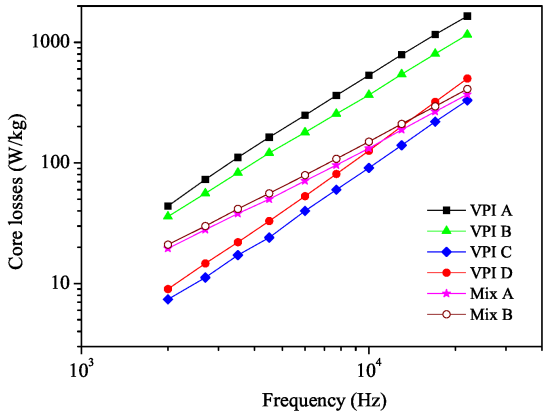

Fig. 7. The dependence of total losses on frequency.

In Fig. 7 the core losses at $B_m = 0.1$ T are plotted vs. frequency, in the frequency range 2–22 kHz. The least steep increase of W_T with frequency was observed in samples with the highest electrical resistivity. We have explained it by the lowest eddy currents during magnetic reversal. The lowest total magnetic losses are observed for the VPI C sample due to the optimal values of the coercivity and the electrical resistivity.

4. Conclusions

The results showed that the resulting soft magnetic properties depend not only on the amount of the electrical-insulating phase, but also on the shape of iron particles, the type of polymer and the preparation method applied. Unfortunately, the high permeability is connected with high core losses and oppositely samples with low core losses exhibit low values of permeability.

Acknowledgments

This work was realized within the frame of projects: ITMS 26220220105 and ITMS 26220120019, supported by Operational Program "Research and Development" financed through European Regional Development Fund; further by Slovak Research and Development Agency under contract APVV-0222-10 and by Scientific Grant Agency of Ministry of Education of Slovak Republic and Slovak Academy of Science — projects VEGA 1/0377/16 and 1/0330/15.

References

[1] H. Shokrollahi, K. Janghorban, *Mater. Sci. Eng. B* **134**, 41 (2006).

[2] K. Asaka, C. Ishihara, *Hitachi Powdered Metals Techn. Rep.* **4**, 3 (2005).

[3] H. Shokrollahi, K. Janghorban, F. Mazaleyrat, M. Lo Buec, V. Ji, A. Tcharkhtchi, *Mater. Chem. Phys.* **114**, 588 (2009).

[4] K.S. Narasimhan, M.L. Marucci, in: *Proc. Conf. Euro PM2003*, Bellstone, Shrewsbury 2003, p. 199.

[5] L.L. Evangelista, D.S. Avila, M.A. Carvalho, H.D. Lopes, P.A.P. Wendhausen, *IEEE Trans. Magn.* **52**, 1 (2016).

[6] A.H. Taghvaei, A. Ebrahimi, M. Ghaffari, K. Janghorban, *J. Magn. Magn. Mater.* **322**, 808 (2010).

[7] R. Bidulský, J. Bidulská, R. de Oro, E. Hryha, M. Maccarini, I. Forno, M. Actis Grande, *Acta Phys. Pol. A* **128**, 647 (2015).

[8] M. Kabátová, E. Dudrová, J. Füzer, J. Füzerová, P. Kollár, *Powder Metall. Progr.* **15**, 23 (2015).

[9] M. Kabátová, J. Füzer, J. Füzerová, E. Dudrová, P. Kollár, *Mater. Sci. Forum* **782**, 533 (2014).

[10] E. Dudrová, M. Kabátová, *Powder Metall.* **59**, 148 (2016).